

Effects of thermal dispersion on heat transfer in cross-flow tubular heat exchangers

Y. Sano, F. Kuwahara, M. Mobedi & A. Nakayama

Heat and Mass Transfer
Wärme- und Stoffübertragung

ISSN 0947-7411

Heat Mass Transfer
DOI 10.1007/s00231-011-0865-
X



Your article is protected by copyright and all rights are held exclusively by Springer-Verlag. This e-offprint is for personal use only and shall not be self-archived in electronic repositories. If you wish to self-archive your work, please use the accepted author's version for posting to your own website or your institution's repository. You may further deposit the accepted author's version on a funder's repository at a funder's request, provided it is not made publicly available until 12 months after publication.

Effects of thermal dispersion on heat transfer in cross-flow tubular heat exchangers

Y. Sano · F. Kuwahara · M. Mobedi ·
A. Nakayama

Received: 22 January 2010 / Accepted: 16 June 2011
© Springer-Verlag 2011

Abstract Effects of thermal dispersion on heat transfer and temperature field within cross-flow tubular heat exchangers are investigated both analytically and numerically, exploiting the volume averaging theory in porous media. Thermal dispersion caused by fluid mixing due to the presence of the obstacles plays an important role in enhancing heat transfer. Therefore, it must be taken into account for accurate estimations of the exit temperature and total heat transfer rate. It is shown that the thermal dispersion coefficient is inversely proportional to the interstitial heat transfer coefficient. The present analysis reveals that conventional estimations without consideration of the thermal dispersion result in errors in the fluid temperature development and underestimation of the total heat transfer rate.

List of symbols

A	Surface area (m^2)
A_{int}	Interface between the fluid and solid (m^2)
a_f	Specific surface area ($1/\text{m}$)
c	Specific heat (J/kgK)
c_p	Specific heat at constant pressure (J/kgK)
C	Size of the touching arm (m)
D	Size of the solid (m)

f, g	Profile functions (–)
H	Size of the cell (m)
hf	Interfacial heat transfer coefficient ($\text{W}/\text{m}^2\text{K}$)
k	Thermal conductivity (W/mK)
n_j	Unit vector pointing outward from the fluid side to solid side (–)
Pr	Prandtl number (–)
q	Heat flux (W/m^2)
T	Temperature (K)
V	Representative elementary volume (m^3)
x_i	Cartesian coordinates (m)
x, y, z	Cartesian coordinates (m)
ε	Porosity (–)
η	Dimensionless vertical coordinate (–)
ρ	Density (kg/m^3)

Special symbols

$\tilde{\phi}$	Deviation from intrinsic average
$\langle \phi \rangle$	Dariclan average
$\langle \phi \rangle^{f,s}$	Intrinsic average

Subscripts and superscripts

f	Fluid
s	Solid

Y. Sano · F. Kuwahara · A. Nakayama (✉)
Department of Mechanical Engineering, Shizuoka University,
3-5-1 Johoku, Naka-ku, Hamamatsu 432-8561, Japan
e-mail: tmanaka@ipc.shizuoka.ac.jp

M. Mobedi
Department of Mechanical Engineering,
Izmir Institute of Technology, Urla 35430, Turkey

A. Nakayama
Department of Civil Engineering, Wuhan Polytechnic
University, Wuhan, Hubei 430023, China

1 Introduction

Thermal dispersion is the spreading of heat caused by variations in fluid velocity about the mean velocity. In addition to the molecular thermal diffusion, there is significant mechanical dispersion in heat and fluid flow in a fluid-saturated porous medium, as a result of hydrodynamic mixing of the interstitial fluid particles passing through pores. This thermal dispersion causes additional heat

transfer, which brings further complications in dealing with transport processes in fluid saturated porous media. As the thermal dispersion becomes significant, the hydrodynamic dispersion comes to play an important role within the pore, resulting an additional flow resistance, which is usually modeled by a velocity square term as in Ergun's equation [1].

In cross flow tubular heat exchangers, the fluids pass through tube bundles. The presence of tubes within the flow field naturally induces significant spreading of heat in both transverse and axial directions. Thus, the effects of thermal dispersion on the heat transfer characteristics are expected to be quite significant. However, in most conventional heat exchanger analyses, such effects have been neglected completely. It should be pointed out that the mixing due to thermal dispersion is much more significant than turbulence mixing. Thus, the thermal dispersion must be considered fully in such heat exchanger analyses.

Yagi et al. [2] were the first to measure the effective longitudinal thermal conductivities of packed bed, taking full account of the effect of thermal dispersion, and eventually found that the longitudinal component of the dispersion coefficient much greater than its transverse component. According to Wakao and Kaguei [3], this great finding, despite of its importance, puzzled them so much that they hesitated to publish their results for some years. Taylor [4] reported a famous analytical treatment in a tube. Since then, a number of theoretical and experimental efforts (e.g. Aris [5], Koch and Brady [6], Han et al. [7], and Vortmeyer [8]) were made to establish useful correlations for estimating the effective thermal conductivities due to thermal dispersion (See Kaviany [9]). Furthermore, Kuwahara et al. [10] and Nakayama et al. [11] conducted a series of numerical experiments by assuming a macroscopically uniform flow through a lattice of rods, so as to elucidate the effects of microscopic velocity and temperature fields on the thermal dispersion. It is also worthwhile to mention that Nakayama et al. [12] derived a thermal dispersion heat flux transport equation from the volume averaged version of Navier–Stokes and energy equations and showed that it naturally reduces to an algebraic expression for the effective thermal conductivity based on a gradient-type diffusion hypothesis.

In this paper, we shall first derive an inverse proportional relationship between the interstitial heat transfer coefficient and the thermal dispersion conductivity, overlooked in the previous investigations. Then, we shall use this relationship to take full consideration of thermal dispersion effects on the temperature field and total heat transfer rate within cross flow tubular heat exchangers. We shall follow the definition of thermal dispersion heat flux to evaluate the longitudinal component of the thermal dispersion conductivity, exploiting the macroscopic energy

equation based on the volume averaging theory. It will be shown that conventional estimations without consideration of the thermal dispersion results in errors in the fluid temperature development and underestimation of the total heat transfer rate.

2 Macroscopic energy equation

Consider a cross flow tubular heat exchanging system as illustrated in Fig. 1. We shall consider the energy equation for the fluid passing through isothermal tubes as follows:

$$\rho_f c_{pf} \frac{\partial T}{\partial t} + \rho_f c_{pf} \frac{\partial}{\partial x_j} u_j T = \frac{\partial}{\partial x_j} \left(k_f \frac{\partial T}{\partial x_j} \right). \quad (1)$$

The boundary conditions are given by

$$x = 0 : \quad T = T_{in} \quad (2a)$$

$$\text{On the tube wall} : \quad T = T_s \quad (2b)$$

such that

$$x = \infty : \quad T = T_s. \quad (2c)$$

We take a local control volume V within in the system, whose length scale $V^{1/3}$ is much smaller than the external characteristic length, but, at the same time, much greater than the structural characteristic length, namely, the tube diameter (see e.g. Nakayama [13]). Under this condition, the volume average of a certain variable ϕ in the fluid phase is defined as

$$\langle \phi \rangle^f \equiv \frac{1}{V_f} \int_{V_f} \phi dV \quad (3)$$

where V_f is the volume space which the fluid phase occupies. The porosity $\varepsilon \equiv V_f/V$ is the volume fraction of

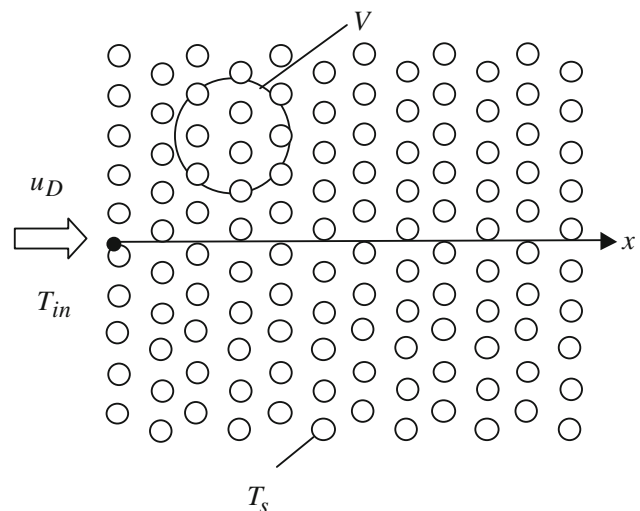


Fig. 1 Cross flow tubular heat exchanger

the fluid space. Following Nakayama [13], Cheng [14], Quintard and Whitaker [15] and many others, we decompose a variable into its intrinsic average and the spatial deviation from it:

$$\phi = \langle \phi \rangle^f + \tilde{\phi}. \tag{4}$$

We shall exploit the following spatial average relationships:

$$\langle \phi_1 \phi_2 \rangle^f = \langle \phi_1 \rangle^f \langle \phi_2 \rangle^f + \langle \tilde{\phi}_1 \tilde{\phi}_2 \rangle^f \tag{5}$$

$$\left\langle \frac{\partial \phi}{\partial x_i} \right\rangle^f = \frac{1}{\varepsilon} \frac{\partial \varepsilon \langle \phi \rangle^f}{\partial x_i} + \frac{1}{V_f} \int_{A_{int}} \phi n_i dA \tag{6}$$

where A_{int} is the local interfacial area between the fluid and solid matrix, while n_i is the unit vector pointing outward from the fluid side to solid side. Similar relationships hold for the solid phase, whose intrinsic average is defined as

$$\langle \phi \rangle^s \equiv \frac{1}{V_s} \int_{V_s} \phi dV. \tag{7}$$

Upon integrating (1) over the local control volume with help of the foregoing relationships, we obtain the volume averaged energy equation as follows:

$$\begin{aligned} & \rho_f c_{pf} \varepsilon \frac{\partial \langle T \rangle^f}{\partial t} + \rho_f c_{pf} \frac{\partial \langle u_j \rangle \langle T \rangle^f}{\partial x_j} \\ &= \frac{\partial}{\partial x_j} \left(\varepsilon k_f \frac{\partial \langle T \rangle^f}{\partial x_j} + \frac{k_f}{V} \int_{A_{int}} T n_j dA - \rho_f c_{pf} \varepsilon \langle \tilde{u}_j \tilde{T} \rangle^f \right) \\ &+ \frac{1}{V} \int_{A_{int}} k_f \frac{\partial T}{\partial x_j} n_j dA \end{aligned} \tag{8}$$

where $\langle u_j \rangle = \varepsilon \langle u_j \rangle^f$ is the Darcian velocity while $\langle T \rangle^f$ is the intrinsic average of the fluid temperature. Obviously, the parenthetical terms on the right hand-side of (8) denote the diffusive heat transfer, while the last term describes the interfacial heat transfer between the tube wall and fluid, which may be modeled via Newton's cooling law [12] as

$$\frac{1}{V} \int_{A_{int}} k_f \frac{\partial T}{\partial x_j} n_j dA = -a_f h_f (\langle T \rangle^f - T_s) \tag{9}$$

where a_f is the specific surface area. The thermal dispersion tensor of our interest may be modeled [12] as

$$-\rho_f c_{pf} \langle \tilde{u}_j \tilde{T} \rangle^f = k_{dis_{sj}} \frac{\partial \langle T \rangle^f}{\partial x_k}. \tag{10}$$

Noting that the surface integral term associated with tortuosity between the parentheses vanishes for isothermal tube walls, we have the following macroscopic energy

equation in terms of the intrinsic average of the fluid temperature, $\langle T \rangle^f$:

$$\begin{aligned} & \rho_f c_{pf} \varepsilon \frac{\partial \langle T \rangle^f}{\partial t} + \rho_f c_{pf} \frac{\partial \langle u_j \rangle \langle T \rangle^f}{\partial x_j} \\ &= \frac{\partial}{\partial x_j} \varepsilon (k_f \delta_{jk} + k_{dis_{jk}}) \frac{\partial \langle T \rangle^f}{\partial x_k} - a_f h_f (\langle T \rangle^f - T_s) \end{aligned} \tag{11}$$

3 Thermal dispersion and interstitial heat transfer

In order to elucidate a close relationship between the longitudinal thermal dispersion conductivity and the interstitial heat transfer coefficient, we shall consider the macroscopic energy equation for the case of steady one dimensional macroscopic flow as illustrated in Fig. 1.

$$\rho_f c_{pf} u_D \frac{d \langle T \rangle^f}{dx} = \frac{d}{dx} \left(\varepsilon k_{dis_{xx}} \frac{d \langle T \rangle^f}{dx} \right) - a_f h_f (\langle T \rangle^f - T_s) \tag{12}$$

where $u_D = \langle u \rangle = \varepsilon \langle u \rangle^f$ is the Darcian axial velocity. The molecular thermal conductivity is dropped since the thermal dispersion overwhelms it. In most conventional heat exchanger analyses, the thermal dispersion term in the foregoing equation is neglected such that

$$\rho_f c_{pf} u_D \frac{d \langle T \rangle^f}{dx} = -a_f h_f (\langle T \rangle^f - T_s) \tag{13}$$

which, with the boundary condition, namely, (2a, 2b, 2c), gives us an exponential temperature distribution:

$$\frac{\langle T \rangle^f - T_s}{T_{in} - T_s} = \exp \left(- \frac{a_f h_f}{\rho_f c_{pf} u_D} x \right). \tag{14}$$

The heat balance relationship given by (14) which neglects the thermal dispersion term is often considered to be valid, when the convection predominates over the heat conduction such as in cross-flow tubular heat exchangers. However, it is the convection from the tube walls that controls the spatial distribution of the local temperature among the tubes and thus enhancing the thermal dispersion activities. Therefore, the effects of the thermal dispersion on the temperature field in reality may never be negligibly small for highly convective flows encountered in heat exchanging systems. Upon replacing the temperature gradient in the diffusion term by the temperature difference using the approximate heat balance relationship (13), we can reduce (12) to an approximate form:

$$\left(\frac{\rho_f c_{pf} u_D}{a_f h_f} + \frac{\varepsilon k_{dis_{xx}}}{\rho_f c_{pf} u_D} \right) \frac{d \langle T \rangle^f}{dx} = -(\langle T \rangle^f - T_s). \tag{15}$$

Thus, the longitudinal thermal dispersion term may be estimated as follows:

$$\begin{aligned}
 -\rho_f c_{p_f} \langle \tilde{u} \tilde{T} \rangle^f &= -\rho_f c_{p_f} \langle u \rangle^f \left(\langle T \rangle^f - \langle T \rangle^s \right) \langle (f-1)(g-1) \rangle^f \\
 &= \left(\frac{(\rho_f c_{p_f} u_D)^2}{\varepsilon a_f h_f} + k_{\text{dis},xx} \right) \langle (f-1)(g-1) \rangle^f \frac{d\langle T \rangle^f}{dx} \quad (16)
 \end{aligned}$$

where the temperature difference is replaced by the temperature gradient using (15). Hence, from (16) and (10), we obtain

$$k_{\text{dis},xx} = \frac{(\rho_f c_{p_f} u_D)^2}{\varepsilon a_f h_f} \frac{\langle (f-1)(g-1) \rangle^f}{1 - \langle (f-1)(g-1) \rangle^f} \quad (17)$$

where

$$u = \langle u \rangle^f f(\eta), \quad (18a)$$

and

$$T - T_s = \left(\langle T \rangle^f - T_s \right) g(\eta). \quad (18b)$$

In order to estimate the coefficient associated with the thermal dispersion conductivity, we shall consider a convective flow through square tubes in a regular arrangement as shown in Fig. 2, where the dimensionless coordinate η is defined as

$$\eta = 2y / (H - D). \quad (19)$$

The profile functions $f(\eta)$ and $g(\eta)$ should satisfy the following conditions:

$$\eta = 0 : \quad \frac{df}{d\eta} = \frac{dg}{d\eta} = 0 \quad (20a)$$

$$\eta = 1 : \quad f = g = 0 \quad (20b)$$

and

$$\langle f \rangle^f = \langle g \rangle^f = 1 \quad (20c)$$

$$\text{where } \langle \phi \rangle^f = \frac{1}{2} \int_{-1}^1 \phi d\eta. \quad (21)$$

Any reasonable functions, which satisfy the foregoing conditions, may be used to evaluate the shape factor $\langle (f-1)(g-1) \rangle^f$. One of the simplest functions would be

$$f(\eta) = g(\eta) = \frac{3}{2} (1 - \eta^2) \quad (22)$$

which gives $\langle (f-1)(g-1) \rangle^f = 1/5$. Hence, we have

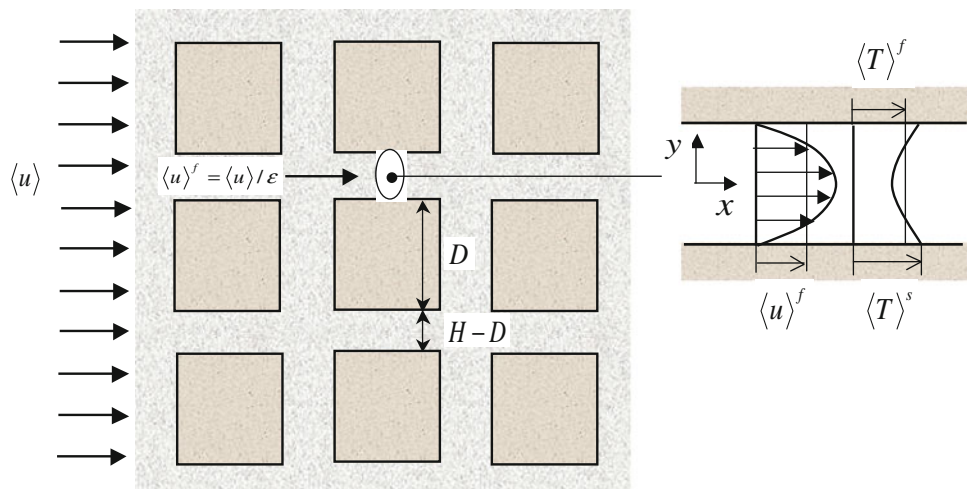
$$k_{\text{dis},xx} = \frac{1}{4} \frac{(\rho_f c_{p_f} u_D)^2}{\varepsilon a_f h_f}. \quad (23)$$

It is interesting to note that the thermal dispersion coefficient, $k_{\text{dis},xx}$ as given by (23), is inversely proportional to the interfacial heat transfer coefficient, h_f . The thermal dispersion coefficient, which is difficult to measure directly, can easily be estimated from (23), as we measure the interstitial heat transfer coefficient instead, using the single-blow method [16]. Alternatively, we may use a number of empirical correlations for the heat transfer coefficient established for tube bundles available in the literature (e.g. Zhukauskas [17]) to estimate the thermal dispersion coefficient. The effects of the tube geometry and arrangement on the thermal dispersion must be accounted by using the heat transfer coefficient obtained for that particular tube geometry and arrangement.

4 Analysis for cross-flow tubular heat exchanger

The validity of the inverse proportional relationship can be checked by carrying out pore scale numerical simulations and evaluating h_f and $k_{\text{dis},xx}$, faithfully following the definitions, namely, (9) and (10), using the pore results obtained using a periodic structure as done by many others

Fig. 2 Model consisting of square tubes for evaluation of the shape factor



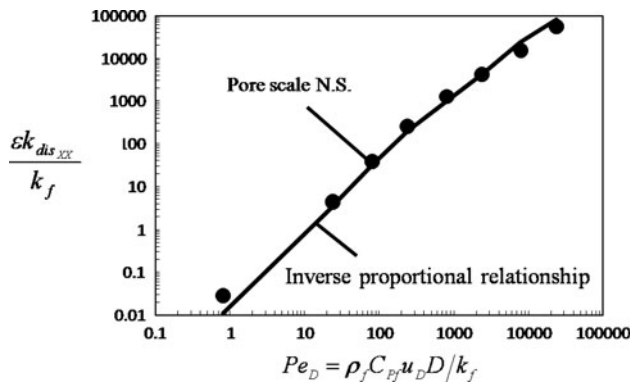


Fig. 3 Comparison of the inverse proportional relationship with DNS

[10, 18, 19]. In Fig. 3, the thermal dispersion conductivity obtained from such pore scale numerical simulations is compared with the thermal dispersion conductivity estimated from the present inverse proportional relationship with the interstitial heat transfer coefficient obtained from the pore scale numerical simulations. The abscissa variable is set to the Peclet number $Pe_D = \rho_f c_{pf} u_D D / k_f$. As the figure shows, the inverse proportional relationship provides a reasonable estimate for the pore scale numerical simulation results, which substantiates the validity of the present relationship.

In what follows, we shall investigate the effects of the thermal dispersion on the temperature field within heat exchangers. Upon substituting (23) for the thermal conductivity into the original macroscopic energy equation, we obtain

$$\rho_f c_{pf} u_D \frac{d\langle T \rangle^f}{dx} = \frac{(\rho_f c_{pf} u_D)^2}{4a_f h_f} \frac{d^2 \langle T \rangle^f}{dx^2} - a_f h_f (\langle T \rangle^f - T_s). \tag{24}$$

The foregoing second order ordinary differential equation may easily be solved with the boundary conditions given by (2a, 2b, 2c) as

$$\begin{aligned} \frac{\langle T \rangle^f - T_s}{T_{in} - T_s} &= \exp\left(-\frac{2(\sqrt{2}-1)a_f h_f x}{\rho_f c_{pf} u_D}\right) \\ &= \exp\left(-0.828 \frac{a_f h_f}{\rho_f c_{pf} u_D} x\right). \end{aligned} \tag{25}$$

Comparison of the foregoing solution (25) with the conventional solution (14) reveals that the conventional solution underestimates the distance required for reaching the thermal equilibrium. For the case of air pre-heater, for example, the temperature at the exit is much lower than the one estimated by the conventional solution neglecting thermal dispersion. The total heat transfer rate may be estimated by integrating (14) and (25) over the distance L as

$$\begin{aligned} Q &= A a_f h_f (T_s - T_{in}) \int_0^L \exp\left(-\frac{a_f h_f}{\rho_f c_{pf} u_D} x\right) dx \\ &= \rho_f c_{pf} u_D A (T_s - T_{in}) \left(1 - \exp\left(-\frac{a_f h_f L}{\rho_f c_{pf} u_D}\right)\right) \end{aligned} \tag{26a}$$

: without dispersion

$$\begin{aligned} Q &= A a_f h_f (T_s - T_{in}) \int_0^L \exp\left(-0.828 \frac{a_f h_f}{\rho_f c_{pf} u_D} x\right) dx \\ &= \frac{\rho_f c_{pf} u_D A (T_s - T_{in})}{0.828} \left(1 - \exp\left(-0.828 \frac{a_f h_f L}{\rho_f c_{pf} u_D}\right)\right) \end{aligned} \tag{26b}$$

: with dispersion.

These two equations indicate that the thermal dispersion works to enhance the total heat transfer from the tubes to fluid. The foregoing (26a, 26b) are valid for all tube geometries and arrangements, as the corresponding heat transfer coefficient is substituted into the equations.

Pore scale numerical simulations were conducted using a semi-finite periodic array of isothermal square tubes, as shown in Fig. 4. Computations were carried out using a grid system, namely, (1000 × 100) to cover one row of the tubes as indicated by the dashed lines. The symmetry boundary conditions were imposed along the horizontal boundaries. Grid nodes are laid out densely around the tubes. The numerical results are found to be independent of any additional refinement of the grid system, thus, ensuring that the results are independent of the number of grid nodes. Convergence was measured in terms of the maximum change in each dimensionless dependent variable during an iteration, which was set to 10⁻⁵.

An air at constant temperature enters into the array of tubes... with $D/H = 0.8$ and $a_f = 4DIH^2$ at $\rho_f c_{pf} u_D D / k_f = 800$ and receives heat from the isothermal tubes. The resulting velocity and temperature fields are presented in Figs. 5 and 6, respectively. As seen from Fig. 5, the velocity field becomes periodically fully-developed quickly after passing through the second unit ($x > 2H$). Since the tubes are closely packed for this case, no separation bubbles are observed behind the tubes. When the

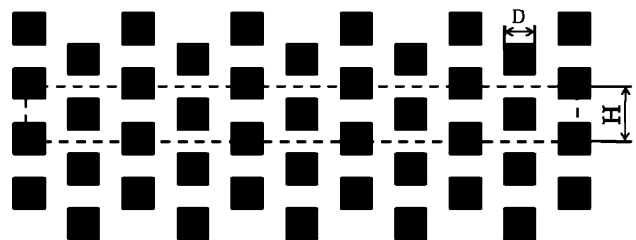


Fig. 4 Physical model for pore scale numerical simulations

Fig. 5 Pore scale velocity field

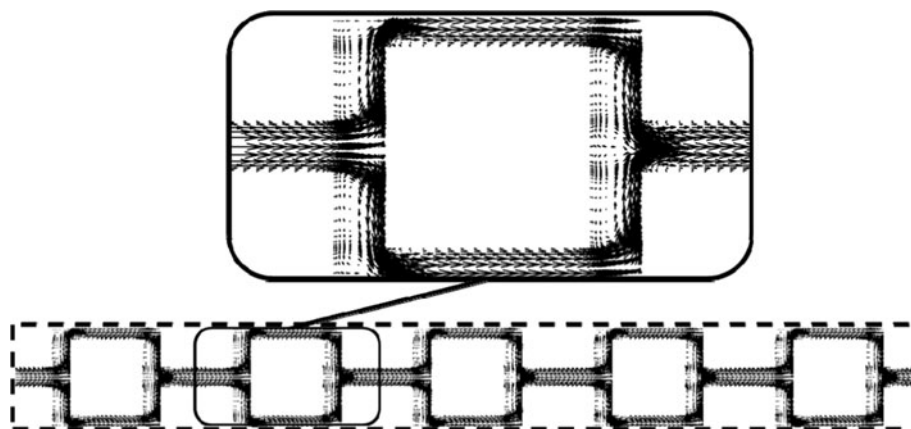
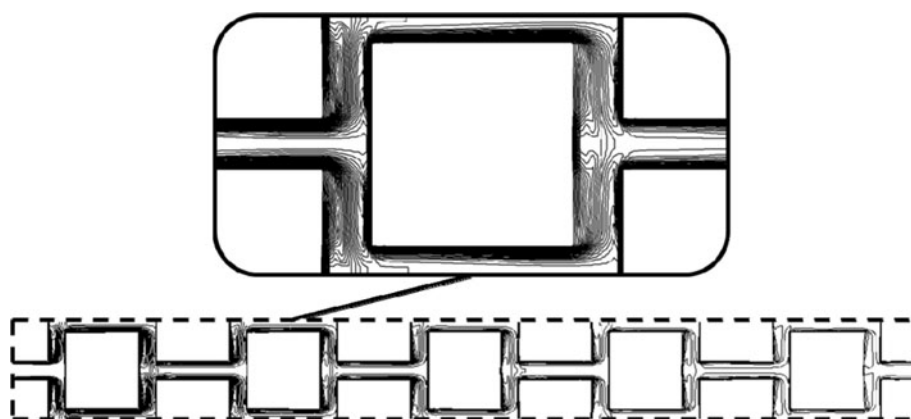


Fig. 6 Pore scale temperature field



porosity is high, the separation bubbles may appear. Such turbulent flow cases may be found in [19].

The pore scale results were integrated over a unit structure to obtain the intrinsic volume average temperature of the fluid $\langle T \rangle^f$. In Fig. 7, the development of the intrinsic volume average temperature obtained from such pore scale numerical simulations is compared with the temperature development estimated from (14) (without

thermal dispersion) and that estimated from (25) (with thermal dispersion). The pore scale numerical results closely follow the temperature variation predicted by (25). Note that the air temperature is substantially lower as we consider thermal dispersion, which guarantees larger temperature difference between the tube and air and hence more heat transfer from the tube to air, as dictated by (26b). This indicates that the effects of thermal dispersion on the temperature development must be taken into full consideration for accurate estimations of the heat transfer characteristics in cross-flow tubular heat exchangers.

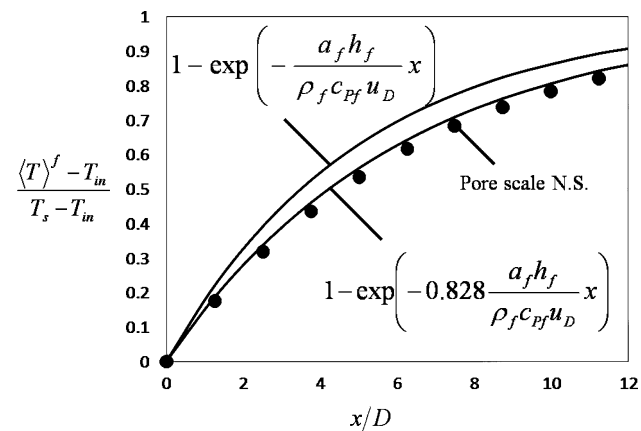


Fig. 7 Development of the fluid temperature

5 Conclusions

An inverse proportional relationship has been found between the interstitial heat transfer coefficient and the longitudinal thermal dispersion conductivity, which was overlooked in most previous investigations. This relationship has been used to obtain a simple analytical expression for the fluid temperature development within cross flow tubular heat exchangers. Pore scale numerical simulations were also conducted to compare the results with the analytical results, revealing that the numerical simulation

results closely follow the temperature development obtained analytically in full consideration of thermal dispersion. The present study clearly indicates that conventional estimations without consideration of the thermal dispersion results in errors in the fluid temperature development and underestimation of the total heat transfer rate.

Acknowledgments The senior author would like to express his sincere thanks to JSPS scholarship program for supporting this study.

References

1. Ergun S (1952) Fluid flow through packed columns. *Chemical Engineering Progress* 48:89–94
2. Yagi S, Kunii D, Wakao N (1960) Studies on axial effective thermal conductivities in packed beds. *AIChE Journal*. 6:543–546
3. Wakao N (1996) Kagueli S. Heat and mass transfer in packed beds. Gordon and Breach, New York
4. Taylor GI (1953) Dispersion of solute matter in solvent flowing slowly through a tube. *Proc. Roy. Soc. London* 15:1787–1806
5. Aris R (1956) On the dispersion of a solute in a fluid flowing through a tube. *Proc R Soc Lond* 235:67–77
6. Koch DL, Brady JF (1985) Dispersion in fixed beds. *J Fluid Mech* 154:399–427
7. Han NW, Bhakta J, Carbonell RG (1985) Longitudinal and lateral dispersion in packed beds: Effect of column length and particle size distribution. *AIChE J* 31:277–288
8. Vortmeyer D (1975) Axial heat dispersion in packed beds. *Chem Eng Sci* 30:999–1001
9. Kaviany M (1991) Principles of heat transfer in porous media. Springer, New York, pp 115–151
10. Kuwahara F, Nakayama A, Koyama H (1996) A numerical study of thermal dispersion in porous media. *Trans ASME J Heat Trans* 118:756–761
11. Nakayama A, Kuwahara F, Umemoto T, Hayashi T (2002) Heat and fluid flow within an anisotropic porous medium. *Trans ASME J Heat Trans* 124:746–753
12. Nakayama A, Kuwahara F, Kodama Y (2006) An equation for thermal dispersion flux transport and its mathematical modelling for heat and fluid flow in a porous medium. *J Fluid Mech* 563:81–96
13. Nakayama A (1995) PC-aided numerical heat transfer and convective flow, CRC Press, Boca, Raton, pp 49–50, 103–115
14. Cheng P (1978) Heat transfer in geothermal systems. *Adv Heat Trans* 14:1–105
15. Quintard M, Whitaker S (1993) One and two equation models for transient diffusion processes in two-phase systems. *Adv Heat Trans* 23:369–465
16. Pucci PF, Horwqard CP, Piersall CH (1967) The single blow transient testing technique for compact heat exchanger surfaces. *J Eng Power Trans ASME* 89:29–40
17. Zhukauskas A (1972) Heat transfer from tubes in crossflow. *Adv Heat Trans* 18:87–159
18. Nakayama A, Kuwahara F, Hayashi T (2004) Numerical modelling for three-dimensional heat and fluid flow through a bank of cylinders in yaw. *J Fluid Mech* 98:139–159
19. Kuwahara F, Yamane T, Nakayama A (2006) Large eddy simulation of turbulent flow in porous media. *Int Comm Heat Mass Transfer* 33:411–418